Simple Space Vector PWM Scheme with Quarter-Wave Symmetric Output Voltage Waveform for Three-Phase Multilevel Inverter

N.N. Lopatkin
Mathematics, physics and informatics department
Shukshin Altai State Humanities Pedagogical University (ASHPU)
Biysk, Russia
nikolay_lopatkin@mail.ru

***Abstract*—The paper describes the simple technique for the quarter-wave symmetric output voltage waveform formation of the three-phase multilevel inverter. This technique is based on the applying the appropriate natural nonsymmetric three-segment vectors switching sequence to the recently proposed simple voltage source multilevel inverter space vector PWM algorithm. Some Mathcad simulated voltages waveforms and loci are shown, and the delta voltage total harmonic distortion (THD) and first three orders n-order integral voltage harmonics factors are presented as the functions of the amplitude modulation index.**

***Keywords*—pulse width modulation inverters; space vector pulse width modulation; total harmonic distortion; multilevel voltage source inverter; voltage space vector PWM of two delta voltages; integer and fractional parts of delta voltages relative values; three-segment vectors switching sequence; voltage waveform quarter-wave symmetry; n-order integral voltage harmonics factors**

I. Introduction

The energy saving in the industry and in the municipal engineering is now often being achieved due to the using the power electronics systems, especially the adjustable frequency induction motor drive for the pumps and fans control. The various types multilevel voltage source inverters (MLVSI) [1, 2] are widely used for the providing both the high quality output AC voltage and the high quality current consumed by the asynchronous motor, at the lowered requirements to the voltage rating of the power switches. Also the increasing role of the MLVSI is obvious from the point of view of the AC voltage generation by the renewable energy sources [3].

The modulation strategy becomes a key factor in the MLVSI output voltage quality improvement [4], providing the enough low value of the power switches commutation frequency and the low level of the corresponding losses.

In engineering practice, the method of the pulse-width modulation (PWM) with the sinusoidal reference (SPWM) and the carrier signals of different levels is being superseded by the space vector (SV) PWM (SVPWM) for the best usage of the input direct voltage, better quality of the output voltage and the best output capability of the inverter, mostly, thanks to the possibility to use some redundant switching states for the MLVSI capacitors voltages balancing [5].

The generated voltage quality is closely related to the waveform symmetry. The three-phase symmetry (TPS) condition is the principal symmetry indicator for the appropriate AC systems, and it can be expressed as follows:

$$u(\omega t)+u(\omega t+2\pi/3)+u(\omega t-2\pi/3)=0\,, \tag{1}$$

here ω is the angular fundamental frequency of the output voltage.

The most of the elaborated and the practice-oriented SVPWM techniques provide the half-wave symmetry (HWS) of the MLVSI instantaneous output voltages waveforms, thereby eliminating the even-order harmonics [6, 1].The HWS corresponds to the condition

$$u(\omega t+\pi)=-u(\omega t)\,. \tag{2}$$

We may say that the HWS has become a conventional attribute of the new proposed modulation schemes. But only a few of the developed SVPWM techniques offer the voltage formation providing the quarter-wave symmetry (QWS), which occurs if the supplementary condition is fulfilled under the appropriate choice of the zero-time reference, besides (2), namely, for an even signal or for an odd signal, respectively:

$$u(-\omega t)=u(\omega t) \text{ or } u(\pi-\omega t)=-u(\omega t)\,, \tag{3}$$

$$-u(\omega t)=u(-\omega t) \text{ or } u(\pi-\omega t)=u(\omega t)\,. \tag{4}$$

Conditions (3) lead to the absence of the sine component in the remaining harmonics, and (4) lead to the absence of the cosine one. As a result, the QWS leads to reduced low order harmonics.

The two-level SVPWM schemes with the QWS are described in [7-11]. The two-level synchronized SVPWM technique [7] is extended to the three-level inverter and shown in [12] as leading to the QWS of the MLVSI output voltage. The new algorithm in [13] is providing this kind of the symmetry due to the modulation index segmentation and the designing the switching sequences specially for each segment. Despite the algorithm is really very interesting and thoroughly developed, it has a high degree of complexity and so it is also limited now by the three-level inverter, like a number of other techniques [1, 14-16].

The general synchronous PWM technique for MLVSI is proposed in [17], however, the QWS output voltages formation is performed without space vectors consideration but via the pulses optimization, which is similar to the used one in the

978-1-5386-1596-6/17/$31.00 ©2017 IEEE

selective harmonic elimination technique (see references in [4]). The main drawback of these two schemes is the increasing computational complexity, which makes a high cost of their applying in high dynamic power systems or becomes the almost insurmountable obstacle for that.

It seems that the reason why the general MLVSI QWS SVPWM algorithm is still absent, is also the increase in the number of computational operations in order to perform the above mentioned symmetry conditions and particularly under the conventional clock cycle symmetric SVPWM pulse patterns implementation.

II. Problem Definition

Our paper [18] offers the simple voltage source multilevel inverter space vector PWM algorithm (based on the oblique-angled coordinates of two delta voltages) with the natural three-segment vectors switching sequence variant providing the instantaneous output voltage quarter-wave symmetry. The voltage waveforms, spectra, total harmonic distortion (THD) and integral factors of harmonics (IHF) comparisons are performed under the same four lowest frequency modulation index values for the before offered nonconventional symmetric five-segment variant and the new offered nonsymmetric three-segment variant of the vectors switching sequence [18, 19].

The principal algorithm is recently proposed [20, 21], it is based on the integer and fractional parts of delta voltages relative values consideration [22, 23], and it has been initially tested on the above mentioned nonconventional symmetric five-segment switching sequence variant [20, 24]. The algorithm can be treated as some symmetric regular sampled SVPWM [6], which is developed on the idea of the oblique-angled coordinates utilization [25].

The integer and fractional parts of the reference delta voltages relative values are used as the coordinates and the duty cycles (over the current clock cycle) of the three nearest space vectors [20, 23, 18].

The QWS voltage formation is based on the appropriate natural nonsymmetric three-segment vectors switching sequence, which is the new and excellent MLVSI switching sequence solution [18].

The main traces of the executed voltage space vector (EVSV) in the context of $\left(u_{ab}^{*}, u_{bc}^{*}\right)$ coordinates are shown in Fig. 1 for the first three rings of triangles. Here dashed lines correspond to the EVSV auxiliary transitions, mostly transitions to the initial triangle vector after next sample inside the same triangle.

The set (in ascending order of the sector number) of the sequences of the being executed vectors inside the triangles for the first ring of modulating triangles is {(1,0),(0,0),(0,1); (0,1),(0,0),(-1,1); (-1,1),(0,0),(-1,0); (-1,0),(0,0),(0,-1); (0,-1),(0,0),(1,-1); (1,-1),(0,0),(1,0)}. With the appearance of the down pointed triangle in the second ring of modulating triangles, the moving of the EVSV endpoint has performed along the zigzag line. So, the set of the vector sequences in sector I of the second ring is {(2,0),(1,0),(1,1); (1,0),(1,1),(0,1); (1,1),(0,1),(0,2)}. The same order is kept at every transition to the subsequent sector. Therefore, the set of the vector sequences in sector II of the second ring is {(0,2),(0,1),(-1,2); (0,1),(-1,2),(-1,1); (-1,2),(-1,1),(-2,2)}, and so on.

As can be seen, every transition to the next ring adds two triangles (one triangle of each type) per sector, keeping both the EVSV trajectory of the moving inside the triangle of each type and the type of the initial (and the final) triangle in each sector.

The purpose of this paper is to describe the details of the simple SVPWM technique for the quarter-wave symmetric output voltage waveform formation of the three-phase MLVSI with equal feeding DC voltage levels [18] and to propose the shortened description for the necessary functions.

III. Delta Voltages SVPWM Algorithm Details

Hereinafter all the inverter phase voltages u_x and delta voltages u_{xy} (including the values with any additional subscript designations) are treated as the relative values that is marked with asterisks:

$$u_x^* = \frac{u_x}{U_d}, \; u_{xy}^* = \frac{u_{xy}}{U_d}, \tag{5}$$

U_d is the direct voltage of the unit (base) level.

The being executed output instantaneous MLVSI delta voltage, formed in accordance with the proposed algorithm, can be expressed as follows:

$$u_{EXExy}^*(t) = \sum_{k=1}^{m_f} u_{kEXExy}^*(t), \tag{6}$$

here $u_{kEXExy}^*(t)$ is the separate instantaneous function (of the current time t), that is defined for its own clock cycle interval having number k,

$$u_{kEXExy}^*(t) = \begin{cases} u_{kEXExy}^*(t_{kc}), \; if \quad (k-1)\cdot T_c < t \le k \cdot T_c, \\ \qquad\qquad\qquad\qquad k = 1,2,\ldots m_f \\ 0, \; otherwise, \end{cases} \tag{7}$$

t_{kc} is the current time from the start of the clock cycle with number k, $t_{kc} = t - (k-1)\cdot T_c$,

T_c is the clock period,

$$u_{kEXExy}^*(t_{kc}) = \lfloor u_{ksREFxy}^* \rfloor + f_{kEXExy}(t_{kc}), \tag{8}$$

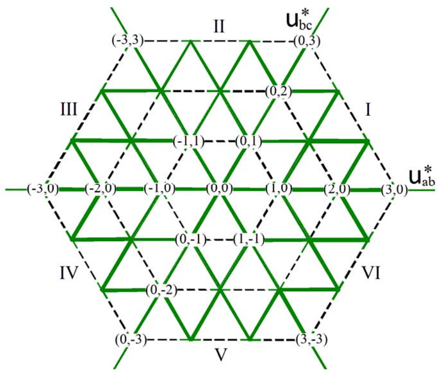

Fig. 1. The traces of the executed voltage space vector under proposed natural switching sequence.

$u^*_{ksREFxy}$ is the sampled, for the k-th clock cycle, value of the corresponding reference delta voltage $u^*_{REFxy}(t)$,

the $\lfloor u^*_{ksREFxy} \rfloor$ and $f_{kEXExy}(t_{kc})$ components nonzero values also exist only within the k-th clock cycle interval,

$\lfloor x \rfloor$ means the rounding down x to the closest integer number, taking into account the sign (the "floor" function), so $\lfloor x \rfloor$ is the integer part of x,

m_f is the frequency modulation index, $m_f = f_c / f$,

f_c and f are, respectively, clock and modulating frequencies, $f_c = 1/T_c$, $f = 1/T$, T is the MLVSI output voltage period.

In accordance with the symmetric regular sampled SVPWM algorithm, the model uses the preliminary sampled values of the reference delta voltages that lead the corresponding formed voltages by the half of the clock cycle, $\frac{360^\circ}{2 \cdot m_f}$, or $\frac{\pi}{m_f}$. So, the sampled values correspond to the initial sinusoidal functions (with the zero phase shift for the voltage $u^*_{EXEbc}(t)$) at the midpoint of the k-th clock cycle:

$$u^*_{ksREFab} = m_a \sin\left((2\pi k - \pi)/m_f + 2\pi/3 \right),$$

$$u^*_{ksREFbc} = m_a \sin\left((2\pi k - \pi)/m_f \right), \tag{9}$$

here m_a is the amplitude modulation index,

$$m_a = \sqrt{3} \cdot U / U_d = \sqrt{3} \cdot U^* = U^*_{\Delta m}, \tag{10}$$

U and U^* are the value and the relative value of the reference space vector magnitude, respectively,

$U^*_{\Delta m}$ is the amplitude relative value of the reference delta voltages.

The Mathcad model lets to generate the time-dependent function for the clock cycle number k:

$$k(t) = \lfloor (t/T - \lfloor t/T \rfloor) \cdot m_f \rfloor + 1 = \left\lfloor \left(\frac{\omega t}{2\pi} - \left\lfloor \frac{\omega t}{2\pi} \right\rfloor \right) \cdot m_f \right\rfloor + 1. \tag{11}$$

This allows considering the functions of the general time course instead of (8) and (9):

$$u^*_{EXExy}(t) = u^*_{\text{int}\,REFxy}(t) + f_{EXExy}(t), \tag{12}$$

here

$$u^*_{\text{int}\,REFxy}(t) = \lfloor u^*_{sREFxy}(t) \rfloor, \tag{13}$$

$$u^*_{sREFab}(t) = m_a \sin\left((2\pi k(t) - \pi)/m_f + 2\pi/3 \right),$$

$$u^*_{sREFbc}(t) = m_a \sin\left((2\pi k(t) - \pi)/m_f \right), \tag{14}$$

$$f_{EXExy}(t) = \sum_{k=1}^{m_f} f_{kEXExy}(t_{kc}). \tag{15}$$

The function $f_{kEXExy}(t_{kc})$ (as well as $f_{EXExy}(t)$) can possess only the values 0 and 1, the clock cycle mean value f_{kEXExy_mean} of this function should correspond to the fractional part of the relative value of the instantaneous reference delta voltage $u^*_{REFxy}(t)$:

$$f_{kEXExy\_mean} = \{ u^*_{ksREFxy} \} = u^*_{ksREFxy} - \lfloor u^*_{ksREFxy} \rfloor. \tag{16}$$

The $f_{kEXExy}(t_{kc})$ and the $f_{EXExy}(t)$ pulses positions on the clock cycle [18, 20] depend on the corresponding voltage $u^*_{EXExy}(t)$ behaviour (see Fig. 1), which is fitting for the accepted switching sequence of the executed vectors. So, for the most part, $f_{kEXExy}(t_{kc})$ formation is the different for the different sectors and triangle types, and it needs the corresponding identifiers [20, 23]. The durations of these pulses (and/or the instants of time of their rising and falling edges) are defined via the fractional values of the relative values of the two delta voltages [23, 20, 18].

IV. Simulation Results

The Mathcad simulated EVSV loci and waveforms of the delta voltage u^*_{EXEbc}, the phase-to-neutral voltage u^*_{EXEan} and the phase-to-ground voltage u^*_{EXEag} are presented in the Table I for the two lowest values of the frequency modulation index. One of the available variants for the directly executed phase-to-ground voltages implementation (having the minimum instantaneous values) is shown here [22, 18].

The generated voltages spectra contain only harmonics (high or low level) of the orders $n = 6 \cdot k \pm 1$, here k belongs to the natural numbers.

The quantitative estimation of the MLVSI output voltage quality has been made via the THD and integral factors of harmonics (IHF) calculation. The n-order voltage IHF index, $\overline{K}^{(n)}_{hu}$, is defined as follows [26]:

$$\overline{K}^{(n)}_{hu} = \frac{\overline{U}^{(n)}_{(hh)}}{\overline{U}^{(n)}_{(1)}} = \frac{\overline{U}^{(n)}_{(hh)} \cdot \omega^n}{U_{(1)}} = \sqrt{\sum_{k=2}^{\infty} \left(\frac{U_{(k)}}{k^n \cdot U_{(1)}} \right)^2}, \tag{17}$$

here $U_{(k)}$, $\overline{U}^{(n)}_{(1)}$ and $\overline{U}^{(n)}_{(hh)}$ are the RMS value of the voltage k harmonic component and RMS values of the results of the n-fold indefinite integral taking of the instantaneous values of the fundamental component $\overline{u}^{(n)}_{(1)}$ and of the high harmonics component $\overline{u}^{(n)}_{(hh)}$ of the whole voltage, correspondingly.

The well-known weighted THD (WTHD) factor [6] completely corresponds to the first order IHF $\overline{K}^{(1)}_{hu}$, and it is the most important index of the IHF family while the current waveform is being estimated via voltage waveform [26].

Here Fig. 2 presents the THD and first to three orders IHF dependences on the amplitude modulation index for the five lowest values of the frequency modulation index: m_f = 12, 18, 24, 30, and 36. As can be seen, the more the m_f value is, the close adjacent to each other curves are situated.

The aggregate indices, taking into account both the voltage harmonics and the number of the switchings in the MLVSI phase leg per the output voltage cycle, are considered in [19].

TABLE I. MATHCAD SIMULATED VOLTAGE WAVEFORMS

m_f	m_a	Executed Voltage Space Vector Locus / Executed Delta Voltage Waveform / Executed Phase-to-Neutral Voltage Waveform / Executed Phase-to-Ground Voltage Waveform
12	0.5	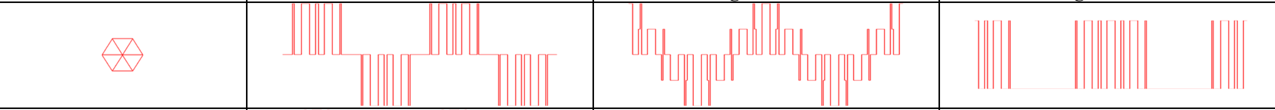
	1.5	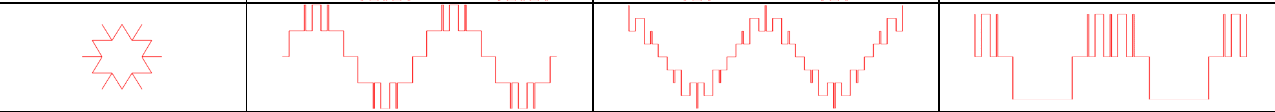
	2.5	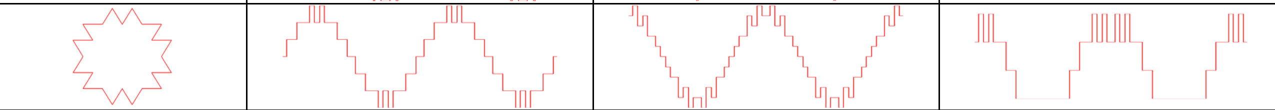
	3.5	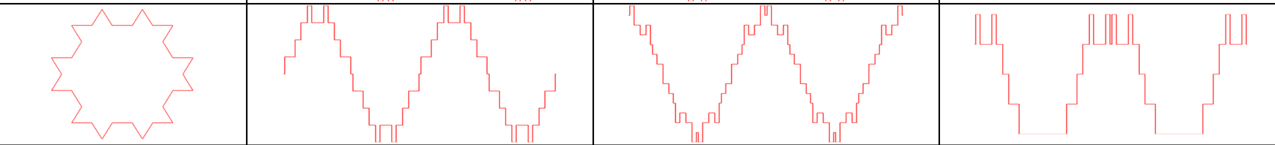
	4.5	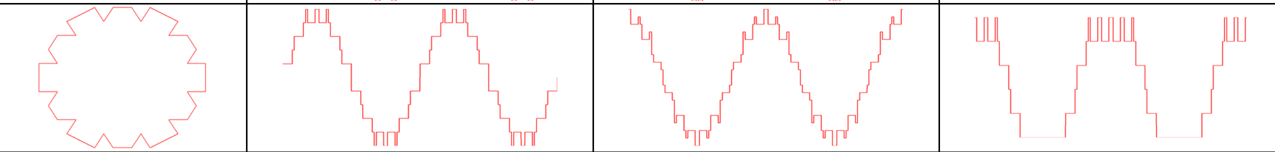
	5.5	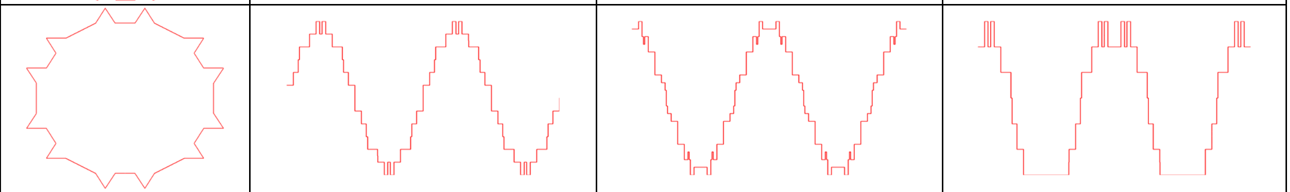
18	0.5	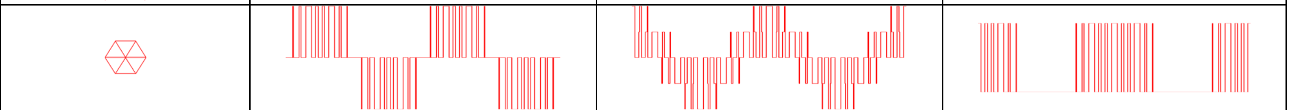
	1.5	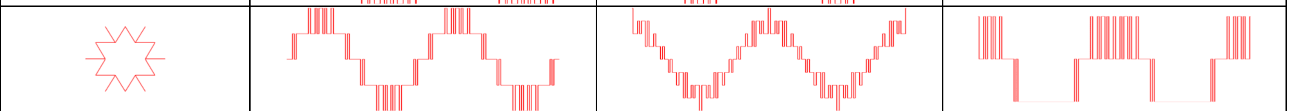
	2.5	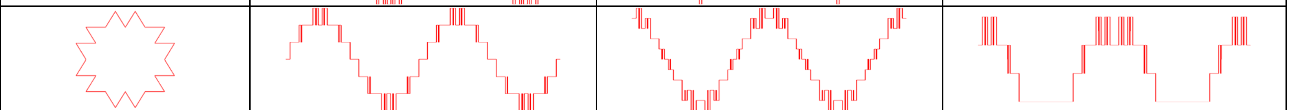
	3.5	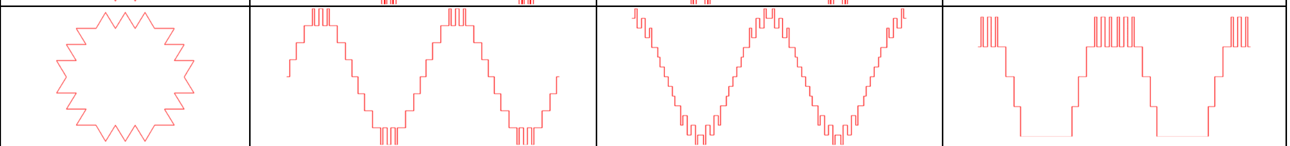
	4.5	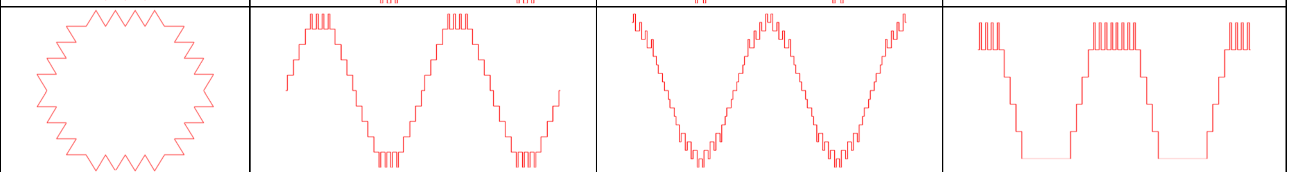
	5.5	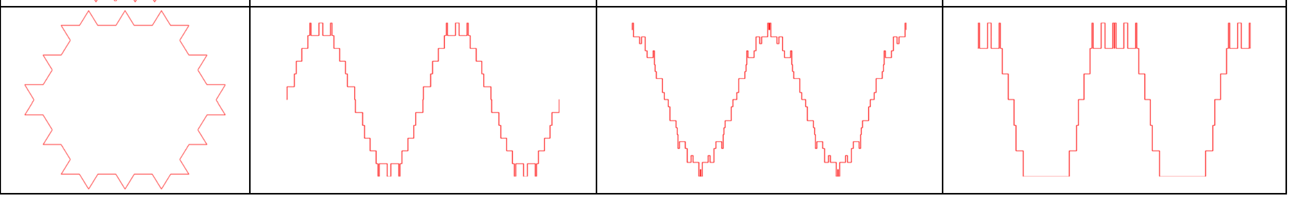

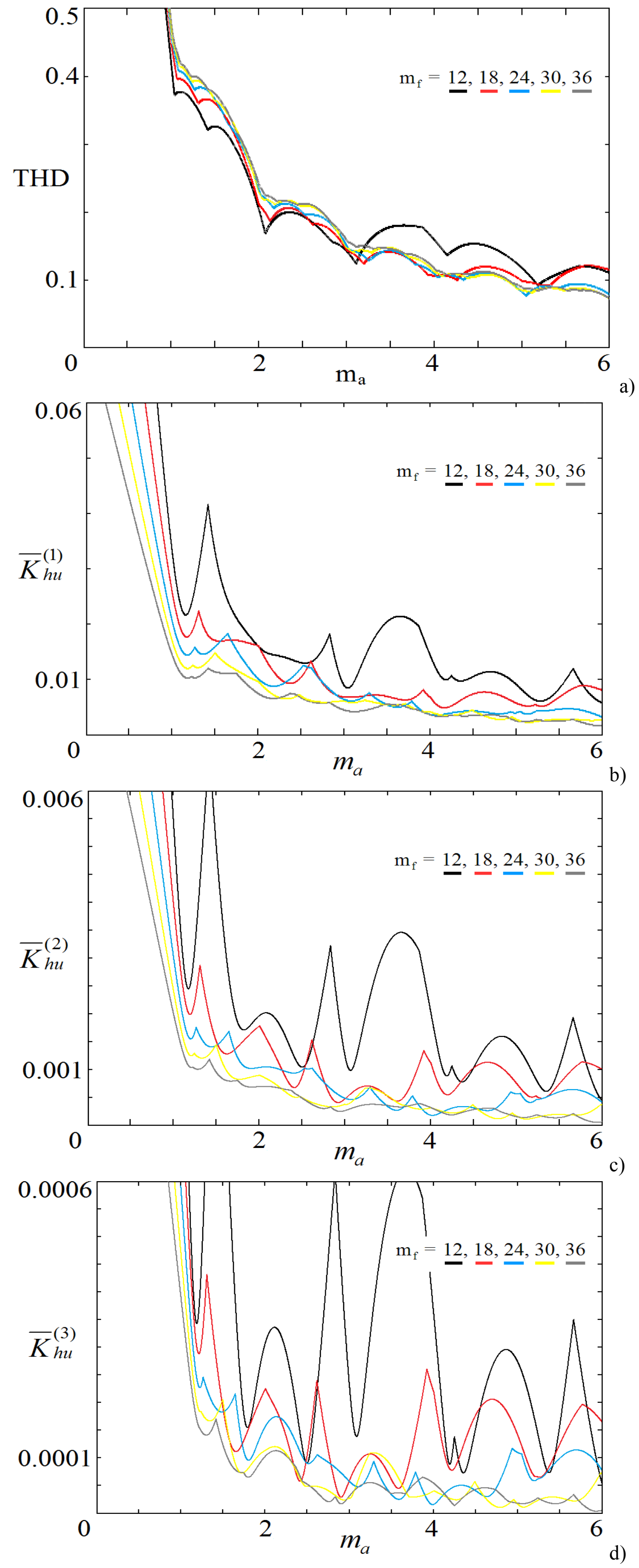

Fig. 2. The Mathcad MLVSI delta voltage THD and integral harmonics factors (IHF) simulation results: a) the zero order IHF (THD); b) the first order IHF; c) the second order IHF; d) the third order IHF.

V. Quarter-Wave Symmetry Conditions and Shortened Functions Description

Simple MLVSI SVPWM algorithm with the proposed natural nonsymmetric three-segment vectors switching sequence produces the delta voltage $u^*_{EXEbc}(t)$, which fulfils conditions (1), (2) and (4), i.e. the TPS, the HWS and the QWS. So, the decomposition (12) lets treat this voltage function as the sum of the two functions (see Fig. 3), also having the waveform quarter-wave symmetry:

$$u^*_{EXEbc}(t) = f_1(t) + f_2(t),$$

$$f_1(t) = u^*_{\text{int } REFbc}(t) + 0.5, \; f_2(t) = f_{EXEbc}(t) - 0.5. \quad (18)$$

Unlike to the function $f_1(t)$, a priori having the constant QWS due to the initial sinusoidal reference and the proper sampling synchronization (see (9)), the function $f_2(t)$ properties strongly depend on the chosen vectors switching sequence. So, just $f_{EXEbc}(t)$ puts the available kind of symmetry. To fulfil the HWS condition (2) and the QWS condition (4) for $f_2(t)$, the corresponding equations should be provided for $f_{EXEbc}(t)$:

$$f_{EXEbc}(\omega t) = 1 - f_{EXEbc}(\omega t - \pi), \quad (19)$$

$$f_{EXEbc}(\omega t) = f_{EXEbc}(\pi - \omega t). \quad (20)$$

As long as the chosen QWS natural three-segment vectors switching sequence is applied, the shortened (to first two sectors) $f_{kEXEbc}(t_{kc})$ description can be used (see Table II), taking into account the QWS, the HWS and also the equations:

$$u^*_{ksREFab} = u^*_{k+m_f/3 \;\; sREFbc}, \; u^*_{EXEab}(t) = u^*_{EXEbc}(t + T/3). \quad (21)$$

VI. Conclusion

The simple SVPWM technique for the quarter-wave symmetric output voltage waveform formation of the three-phase MLVSI with equal feeding DC voltage levels is presented, which is avoiding a symmetric vectors switching sequence and thereby reducing the per phase switchings number of the power semiconductor switches.

In addition to the voltage harmonics factors dependences on the amplitude modulation index, some quarter-wave symmetry conditions of the algorithm, and the shortening of the functions description, which is related to the symmetry, are shown.

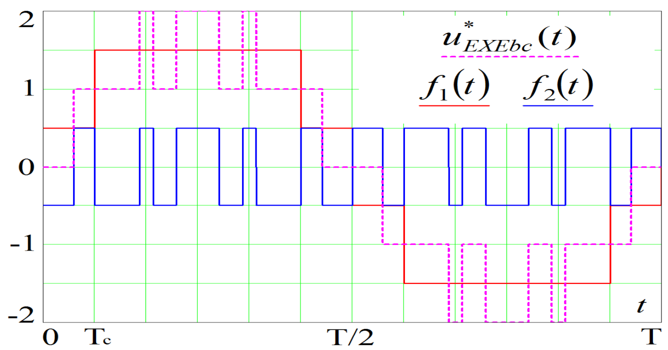

Fig. 3. The MLVSI executed delta voltage and its component functions Mathcad simulated waveforms under m_f = 12, m_a = 1.6.

TABLE II. FRACTIONAL COMPONENT FUNCTION FOR SECTORS I AND II

Sector	Triangle Type and EVSV Trajectory	Fractional Component Function of Executed Delta Voltage on k-th Clock Cycle, $f_{kEXEbc}(t_{kc})$
I 0°…60°	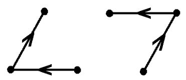	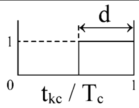 t_{kc} / T_c $d = \{u^*_{ksREFbc}\}$
II 60°…120°	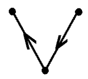	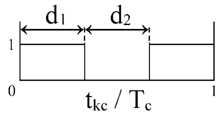 t_{kc} / T_c $d_1 = \{u^*_{ksREFab}\} + \{u^*_{ksREFbc}\} - 1$ $d_2 = 1 - \{u^*_{ksREFbc}\}$
	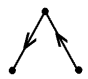	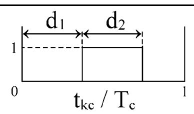 t_{kc} / T_c $d_1 = \{u^*_{ksREFab}\}$ $d_2 = \{u^*_{ksREFbc}\}$

REFERENCES

[1] Bin Wu, M. Narimani, High-Power Converters and AC Drives. Second Edition. Wiley-IEEE Press, 2017.

[2] S. Kouro, M. Malinowski, K. Gopakumar, J. Pou, L.G. Franquelo, Bin Wu, J. Rodriguez, M.A. Pérez, J.I. Leon, “Recent advances and industrial applications of multilevel converters,” IEEE Transactions on Industrial Electronics, Vol. 57, Iss. 8, August 2010, pp. 2553-2580.

[3] F.L. Luo, H. Ye, Advanced DC/AC Inverters: Applications in Renewable Energy. CRC Press, 2013.

[4] J.I. Leon, S. Kouro, J. Rodriguez, Bin Wu, “The essential role and the continuous evolution of modulation techniques for voltage-source inverters in the past, present, and future power electronics,” IEEE Transactions on Industrial Electronics, Vol. 63, Iss. 5, May 2016, pp. 2688-2701.

[5] S.A. Gonzalez, S.A. Verne, M.I. Valla, Multilevel Converters for Industrial Applications. CRC Press, 2013.

[6] D.G. Holmes, T.A. Lipo, Pulse Width Modulation for Power Converters. Piscataway, NJ: IEEE Press, 2003.

[7] V. Oleschuk, F. Blaabjerg, “Synchronized scheme of continuous space-vector PWM with the real-time control algorithms,” PESC 04, 2004 IEEE 35th Annual Power Electronics Specialists Conference, Germany, Aachen, June 20-25, 2004. Proceedings, Vol. 2, pp. 1207-1213.

[8] G. Narayanan, V.T. Ranganathan, “Two novel synchronized bus-clamping PWM strategies based on space vector approach for high power drives,” IEEE Transactions on Power Electronics, Vol. 17, Iss. 1, January 2002, pp. 84-93.

[9] A. Mehrizi-Sani, S. Filizadeh, “An optimized space vector modulation sequence for improved harmonic performance,” IEEE Transactions on Industrial Electronics, Vol. 56, Iss. 8, August 2009, pp. 2894-2903.

[10] J. Biswas, M.D. Nair, V. Gopinath, M. Barai, “An optimized hybrid SVPWM strategy based on multiple division of active vector time (MDAVT),” IEEE Transactions on Power Electronics, Vol. 32, Iss. 6, June 2017, pp. 4607-4618.

[11] S. Jung, J. Park, J.-Ik Ha, “Synchoronous PWM with single voltage vector per sector in voltage source inverter,” ECCE 2015, 2015 Seventh Annual IEEE Energy Conversion Congress and Exposition (ECCE), Montreal, Canada, 20-24 September, 2015. Proceedings, pp 4012-4018.

[12] V. Oleschuk, V. Ermuratskii, F. Barrero, “Analysis and synthesis of symmetrical output voltage of three-level converters with space-vector PWM,” Tekhnichna Elektrodynamika (Technical Electrodynamics), Institute of electrodynamics NAS of Ukraine, Kyiv, Iss. 5, 2016, pp. 17-19. (In Russian).

[13] W. Chen, H. Sun, X. Gu, and C. Xia, “Synchronized space vector PWM for three level VSI with lower harmonic distortion and switching frequency,” IEEE Transactions on Power Electronics, Vol. 31, Iss. 9, September 2016, pp. 6428-6441.

[14] A.R. Beig, G. Narayanan, V.T. Ranganathan, “Modified SVPWM algorithm for three level VSI with synchronized and symmetrical waveforms,” IEEE Transactions on Industrial Electronics, Vol. 54, Iss. 1, February 2007, pp. 486-494.

[15] A.R. Beig, S. Kanukollu, K. Al Hosani, A. Dekka, “Space-vector-based synchronized three-level discontinuous PWM for medium-voltage high-power VSI,” IEEE Transactions on Industrial Electronics, Vol. 61, Iss. 8, August 2014, pp. 3891-3901.

[16] G. Vivek, M.D. Nair, M. Barai, “Experimental study on SVPWM switching sequences for VSIs,” IEEE - PEMC 2016, 2016 IEEE 17th International Conference on Power Electronics and Motion Control (PEMC), Varna, Bulgaria, 25-28 September, 2016. Proceedings, pp. 92-97.

[17] A.K. Rathore, J. Holtz, T. Boller, “Synchronous optimal pulsewidth modulation for low-switching-frequency control of medium-voltage multilevel inverters,” IEEE Transactions on Industrial Electronics, Vol. 57, Iss. 7, July 2010, pp. 2374-2381.

[18] N.N. Lopatkin, “Voltage quality comparison of space vector PWM voltage source multilevel inverter under symmetric and nonsymmetric switching sequence variants: voltage waveforms, spectra and THD,” ICIEAM-2017, 2017 3rd International Conference on Industrial Engineering, Applications and Manufacturing (ICIEAM). IEEE Conference # 40534. Peter the Great Saint-Petersburg Polytechnic University. Russia, St. Petersburg, May 16-19, 2017. Proceedings. Paper 3.4.58 (pp. 1-8), in press.

[19] N.N. Lopatkin, G.S. Zinoviev, “Voltage quality comparison of space vector PWM voltage source multilevel inverter under symmetric and nonsymmetric switching sequence variants: voltage harmonics integral factors,” ICIEAM-2017, 2017 3rd International Conference on Industrial Engineering, Applications and Manufacturing (ICIEAM). IEEE Conference # 40534. Peter the Great Saint-Petersburg Polytechnic University. Russia, St. Petersburg, May 16-19, 2017. Proceedings. Paper 3.4.59 (pp. 1-7), in press.

[20] N.N. Lopatkin, “Simple delta voltages space vector PWM algorithm for voltage source multilevel inverters,” 2016 2-nd International Conference on Intelligent Energy and Power Systems (IEPS), Kyiv, Ukraine, June 7-11, 2016. Conference Proceedings, IEEE Catalog Number: CFP1605X-PRT. ISBN: 978-1-5090-1767-6, pp. 149-154.

[21] N.N. Lopatkin, “Output voltage simulation of multilevel inverter with space vector modulation of two delta voltages,” Tekhnichna Elektrodynamika (Technical Electrodynamics), Institute of Electrodynamics NAS of Ukraine, Kyiv, Iss. 5, 2016, pp. 20-22. (In Russian).

[22] N.N. Lopatkin, “Representation of the voltage space vector of the multilevel inverter in oblique-angled coordinate systems of two delta voltages,” APEIE-2014, 12th International Conference on Actual Problems of Electronic Instrument Engineering (APEIE – 34006), Novosibirsk, 2-4 October, 2014. Proceedings, Vol. 1, pp. 824-828.

[23] N.N. Lopatkin, “Some new representations of the multilevel inverter voltage space vector in the complex plane,” SIBCON-2015, 2015 International Siberian Conference on Control and Communications (SIBCON), Russia, Omsk, May 21-23, 2015. Proceedings, IEEE Catalog Number: CFP15794-CDR. ISBN: 978-1-4799-7102-2, 222em.pdf.

[24] N.N. Lopatkin, “Voltage harmonics integral factors estimation of multilevel inverter with space vector modulation of two delta voltages,” APEIE-2016, 13th International Conference on Actual Problems of Electronic Instrument Engineering (APEIE – 39281), Novosibirsk, 3-6 October, 2016. Proceedings, Vol. 1, part 3, pp. 112-115.

[25] N. Celanovic, D. Boroyevich, “A fast space-vector modulation algorithm for multilevel three-phase converters,” IEEE Transactions on Industry Applications, Vol. 37, Iss. 2, March/April 2001, pp. 637-641.

[26] G.S. Zinoviev, Power Electronics. Textbook for undergraduate students. Fifth edition. Moscow: Jurajt, 2012. 667 p. (In Russian).